Suppression of Na interstitials in Na-F codoped ZnO

Wenxing Huo, Zengxia Mei, Aihua Tang, Huili Liang, and Xiaolong Du

Citation: Journal of Applied Physics **123**, 161403 (2018); doi: 10.1063/1.5003475
View online: https://doi.org/10.1063/1.5003475
View Table of Contents: http://aip.scitation.org/toc/jap/123/16
Published by the American Institute of Physics

Suppression of Na interstitials in Na-F codoped ZnO

Wenxing Huo,[1,2] Zengxia Mei,[1,a)] Aihua Tang,[1,2] Huili Liang,[1] and Xiaolong Du[1,2,a)]
[1]*Key Laboratory for Renewable Energy, Institute of Physics, Chinese Academy of Sciences, Beijing 100190, China*
[2]*School of Physical Sciences, University of Chinese Academy of Sciences, Beijing 100049, China*

(Received 6 September 2017; accepted 8 February 2018; published online 28 February 2018)

Controlling the formation of interstitial Na (Na_i) self-compensating defects has been a long-term physics problem for effective Na doping in ZnO. Herein, we present an experimental approach to the suppression of Na_i defects in ZnO via Na and F codoping under an oxygen-rich condition during the molecular beam epitaxy growth process. It is found that the incorporation of such large numbers of Na and F dopants ($\sim 10^{20}\,cm^{-3}$) does not cause an obvious influence on the lattice parameters. Hall-effect measurements demonstrate that F doping efficiently raises the Fermi level (E_F) of ZnO films, which is expected to make the formation energy of Na_i and Na_{Zn} increase and decrease, respectively. Most of the Na atoms occupy the substitutional Zn sites, and the formation of Na_i is suppressed consequently. Secondary ion mass spectrometry measurements reveal that F and Na atoms are tightly bonded together due to their strong Coulomb interaction. The enhanced deep level emission (DLE) in ZnO:Na-F is ascribed to the considerable amount of isolated Zn vacancy (V_{Zn}) defects induced by the elevated E_F and the formation of neutral $\left(F_O^+ - Na_{Zn}^-\right)^0$ complexes. On the other hand, formation of $\left(F_O^+ - V_{Zn}^{2-}\right)^-$ complexes in ZnO:F exhausts most of the isolated Zn vacancies, leading to the disappearance of the DLE band. *Published by AIP Publishing.*
https://doi.org/10.1063/1.5003475

I. INTRODUCTION

Zinc oxide, with a wide band gap of 3.37 eV and a large exciton binding energy of 60 meV, is regarded as a highly prospective semiconductor material for electronic and optoelectronic device applications, especially ultraviolet (UV) light-emitting diodes and laser diodes.[1,2] However, the prospect of using ZnO as a complement or alternative to GaN has long been impeded by the difficulties in producing stable and reproducible p-type ZnO. Substitutional Na (Na_{Zn}) is proposed as the most promising shallow acceptor in ZnO, but its low solid solubility and the by-product of Na doping, a considerable number of interstitial Na (Na_i) self-compensating centers, severely restrain the p-type doping efficiency.[3] Shen *et al.* investigated the effect of Na_{Zn}/Na_i ratio (r) on the electrical properties of Na-doped ZnO thin films and found that the electron concentration increased continuously when $r < 1$.[4] Thus, the key issue for effective Na doping is to suppress the formation of Na_i. To solve this problem, Lee and Chang proposed that codoping with H would significantly enhance the solubility of Na_{Zn} from 10^{17} to $10^{20}\,cm^{-3}$ while suppressing the formation of Na_i.[5] It was supposed that incorporation of H will lead to an elevation of the Fermi level (E_F), and the formation energy of Na_i will hence be increased, while that of Na_{Zn} will be decreased. Recently, an experimental implementation of Na-H codoping was performed by utilizing NaOH as the dopant of Na and H, and a weak p-type conductivity was obtained with a hole concentration of $2.6 \times 10^{16}\,cm^{-3}$.[6]

Meanwhile, Yamamoto and Katayama-Yoshida have theoretically proposed a Li and F codoping method,[7] and Chen *et al.* further predicted the suppression of interstitial Li with the presence of F atoms under O-rich conditions.[8] It is well known that F donors efficiently occupy the substitutional sites of O. By raising the E_F of ZnO films close to the conduction band minimum via F doping, the formation energy of Na_{Zn} is expected to be lowered as well, similar to the case of Li-F codoping. Considering a similar ionic radii of F and O (F^- 133 pm, O^{2-} 140 pm),[9] the lattice distortion induced by F-doping can be ignored.[10] Furthermore, F anions can passivate surface dangling bonds and diminish O-related defects, leading to higher growth rates and better crystalline qualities,[11–13] which will balance the mobility deterioration caused by Na dopants.[4] Herein, the effect of Na-F codoping in ZnO films on the suppression of Na_i is experimentally investigated by radio-frequency plasma assisted molecular beam epitaxy (rf-MBE), combined with the X-ray diffraction technique (XRD), X-ray photoelectron spectroscopy (XPS), Hall-effect, temperature-dependent Hall (TDH) measurement, secondary ion mass spectrometry (SIMS), and low-temperature photoluminescence (LT-PL) techniques.

II. EXPERIMENTAL

A. Film growth

Undoped, F-doped (ZnO:F), and Na-F codoped (ZnO:Na-F) ZnO single crystalline thin films are synthesized on undoped ZnO/MgO/α-Al_2O_3 templates by rf-MBE. More growth details about the undoped ZnO templates (160 nm) can be found elsewhere.[14,15] The epilayers are deposited at

a)Authors to whom correspondence should be addressed: zxmei@iphy.ac.cn and xldu@iphy.ac.cn

450 °C under O-rich conditions, where the rf-power is 340 W and the oxygen flux is 2.6 standard cubic centimeter per minute (sccm). The epitaxy temperature is chosen to balance the crystal quality and doping efficiency, since ZnO films grown at low temperatures exhibit a rough surface and poor crystal quality,[16] while a large number of F atoms will escape at high temperature.[12] Solid anhydrous ZnF_2 (4N5) and NaOH (5N) are used as the sources of F and Na elements, and their K-cell temperature is kept at 580 °C and 400 °C, respectively. The thickness of undoped ZnO, ZnO:F, and ZnO:Na-F epilayers is 210 nm, 280 nm, and 140 nm, respectively.

B. Characterization

The crystal structure of the films is investigated by XRD (SmartLab, Rigaku). The surface morphology and roughness are evaluated by using commercial atomic force microscopy (AFM, MultiMode 8, Bruker). The chemical states of F and Na are analyzed by XPS (ESCALAB 250X, ThermoFisher Scientific) with a monochromatic Al Kα source (1486.6 eV). Their concentration depth profiles are obtained with SIMS (MAXIM SIMS/SNMS Workstation, Hiden Analytical). The film thickness and the depth of the crater sputtered by SIMS are measured by a surface profiler (KLA-Tencor P-6). The electrical properties are revealed by using the Van der Pauw method (HMS-3000, Ecopia at room temperature and PPMS-9T, Quantum Design over 2–300 K). LT-PL measurements are carried out on a high-resolution confocal-microscope Raman spectroscope (Horiba HR Evolution, 325 nm He-Cd laser) at 77 K.

III. RESULTS AND DISCUSSION

A. Structural characterization

The conventional XRD θ–2θ scan curves of undoped ZnO, ZnO:F, and ZnO:Na-F are shown in Fig. 1(a). The raw data is analyzed by the PowderX software.[17] No other peaks except those of ZnO and Al_2O_3 are detected in all samples, indicating a preferred c-axis orientation and single wurtzite structure without any undesired F or Na related phases. To determine the lattice parameters, θ–2θ scans in an asymmetric diffraction configuration are performed, as shown in Fig. 1(b). In all samples, the ZnO (002) and (103) peaks conformably locate at 34.44° and 62.87°, respectively. The lattice parameters a and c are calculated by the following formula:[18]

$$\sin^2\theta = \frac{\lambda^2}{4}\left(\frac{4}{3}\frac{h^2+hk+k^2}{a^2}+\frac{l^2}{c^2}\right), \quad (1)$$

where λ is the wavelength of the X-ray radiation (0.15406 nm for Cu Kα). The resulting values are $a = 0.3250$ nm and $c = 0.5204$ nm, in good accordance with the bulk values.[19] Meanwhile, the same lattice constants of these samples indicate that the amount of Na_i is below the sensitivity of the XRD instrument.[20,21]

The full width at half maximum (FWHM) values of ZnO (002) peaks are extracted from the rocking curves, as shown in Fig. 1(c). The relatively large FWHM value of the undoped ZnO is due to the inferior quality at low growth temperature.[16] The smaller FWHM values of ZnO:F and ZnO:Na-F with respect to that of undoped ZnO indicate their better crystalline qualities. This result is in accordance with the surface morphology characterization gained by AFM (not shown here). The root mean square roughness (RMS) extracted from 10×10 μm^2 images is 18.7 nm, 5.43 nm, and 10.3 nm for undoped ZnO, ZnO:F, and ZnO:Na-F, respectively. The surface of ZnO thin films becomes smoother after F doping or

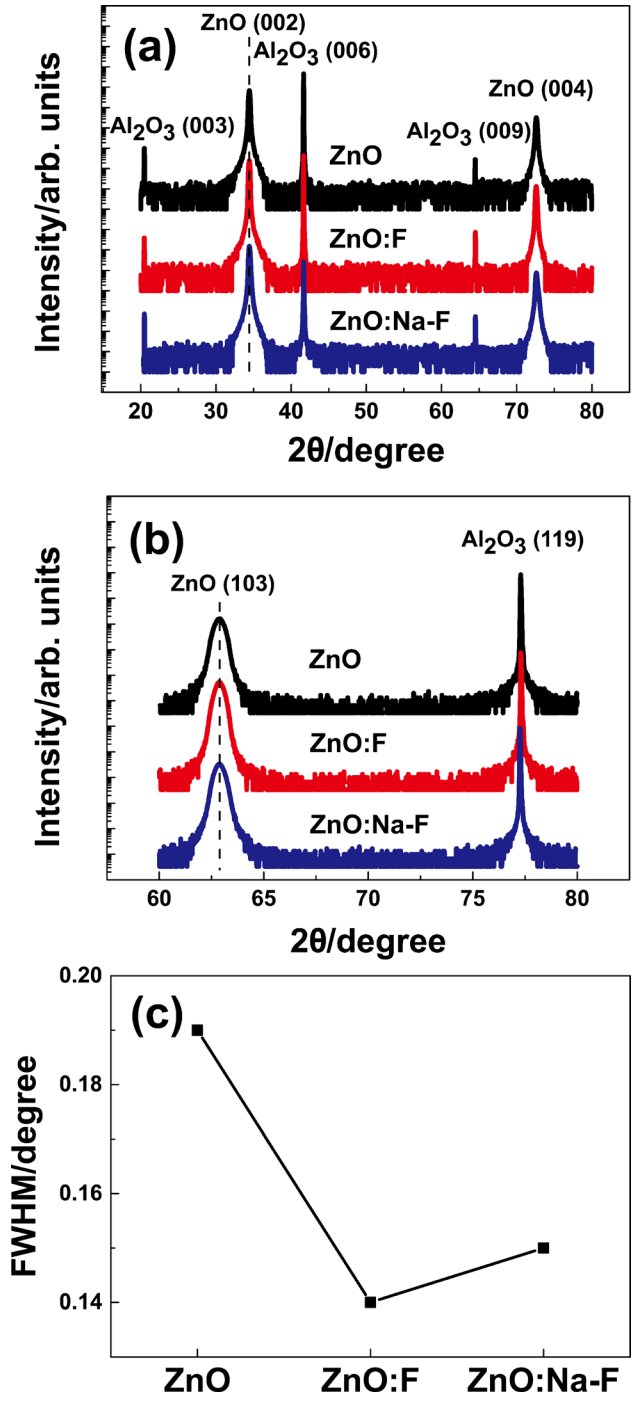

FIG. 1. XRD results of undoped ZnO, ZnO:F, and ZnO:Na-F thin films: θ-2θ scans in (a) symmetric and (b) asymmetric diffraction configurations, and (c) FWHM values of ZnO (002) peaks.

Na-F codoping. Passivation of surface dangling bonds and diminishment of O-related defects by F anions contribute to the better crystalline quality and smoother surface.

B. Compositional characterization

XPS measurements are adopted to validate the existence of F and Na dopants and their chemical states. F 1s and Na 1s spectra of ZnO:F and ZnO:Na-F thin films are shown in Figs. 2(a) and 2(b), respectively. The F 1s signal is not detected in ZnO:F despite a high doping concentration above $1 \times 10^{20}\,\mathrm{cm}^{-3}$ (see Sec. III E for the dopant concentration), while it appears in ZnO:Na-F (685.3 eV), indicating a higher concentration of F in ZnO:Na-F than that in ZnO:F. The presence of sodium in ZnO:Na-F is illustrated in Fig. 2(b) with a clear Na 1s peak (1071.6 eV), which is attributed to the Na-O bond.[22] The peak related to Na_i is not observed,[4] suggesting that most Na dopants are in the form of Na_{Zn} rather than Na_i. Considering the 0.1% detection limit and the elemental sensitivity factor in the XPS instrument, the Na concentration in this sample is estimated to be $>8.56 \times 10^{19}\,\mathrm{cm}^{-3}$. Such a large number of Na acceptors would greatly compensate the electrons donated by F donors.

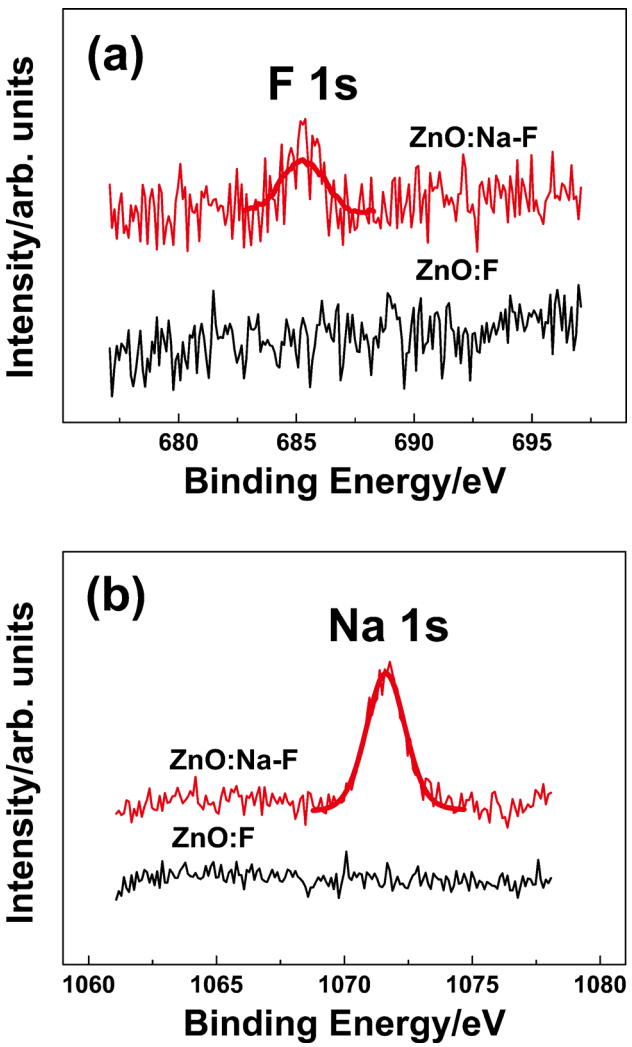

FIG. 2. XPS spectra of ZnO:F and ZnO:Na-F thin films: (a) F 1s and (b) Na 1s.

To further explore the dopant concentration and distribution in ZnO:F and ZnO:Na-F, SIMS analyses of F and Na depth profiles are performed [Fig. 3]. It should be noted that H element is not detectable in all samples due to the sensitivity of the facility. As illustrated in Fig. 3(a), the average intensity of F in the epilayer of ZnO:Na-F is higher than that in ZnO:F, which is consistent with the XPS results. The distribution of F in these two epilayers is remarkably different—it is basically uniform in ZnO:F, but manifests a peak-valley shape in ZnO:Na-F. Intriguingly, Na exhibits almost the same distribution as F in ZnO:Na-F, as shown in Fig. 3(b). The intensities of Na and F are normalized for clarity. The nearly overlapped profiles suggest that the positions of F and Na atoms are very close, which should be the result of their strong Coulomb interaction and tight bonding. The behavior is very typical for the Na-F codoped samples. The unusual peak-valley shaped profiles of Na and F have not been well interpreted and need to be further studied.

C. Electrical properties

Hall measurement results of these samples are summarized in Table I. Note that the thickness data used for the calculation of electrical properties are those of the doped layers

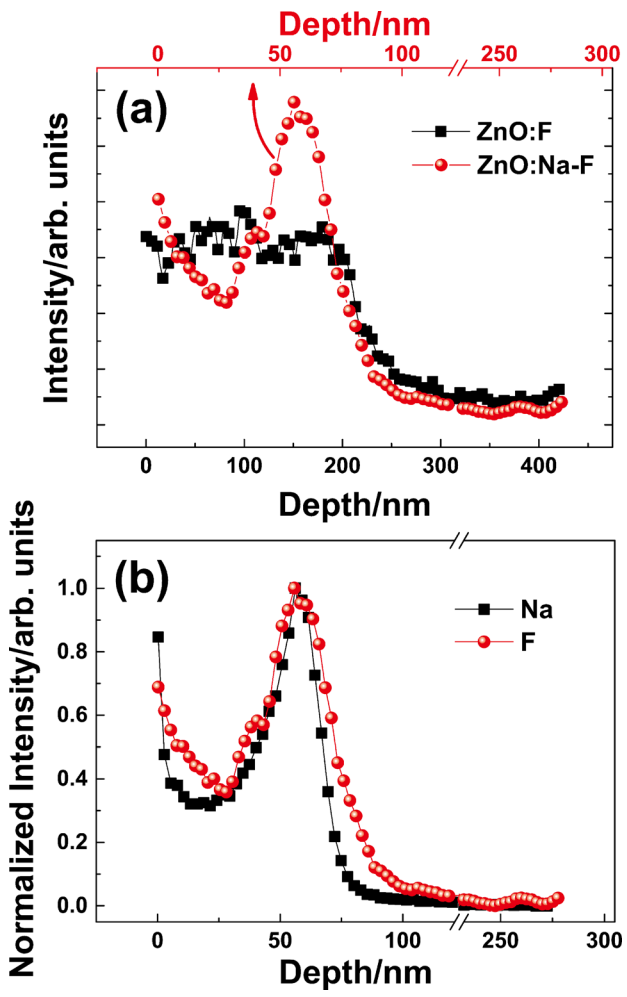

FIG. 3. SIMS profiles: (a) depth profiles of the F element in ZnO:F and ZnO:Na-F thin films and (b) normalized intensities vs. depth profiles of Na and F elements in the ZnO:Na-F thin film.

TABLE I. Hall data of undoped ZnO, ZnO:F, and ZnO:Na-F thin films.

Samples	Thickness (nm)	Electron concentration (cm^{-3})	Mobility ($cm^2\ V^{-1}\ s^{-1}$)	Resistivity (Ω cm)
ZnO	370	3.297×10^{17}	22.22	8.520×10^{-1}
ZnO:F	280	1.115×10^{20}	70.91	7.902×10^{-4}
ZnO:Na-F	140	1.314×10^{18}	63.07	7.533×10^{-2}

in ZnO:F and ZnO:Na-F samples. All the samples exhibit n-type conductivity, but the electron concentrations (n) significantly depend on the dopants. When ZnO is doped with a high dose of F, n reaches $1.115 \times 10^{20}\,cm^{-3}$, more than two orders of magnitude higher than that of undoped ZnO. Obviously, ZnO:F is highly degenerate. Interestingly, n decreases to $1.314 \times 10^{18}\,cm^{-3}$ for ZnO:Na-F, almost two orders of magnitude lower than that of ZnO:F. The mobility (μ) is greatly enhanced after F and Na-F doping, which is quite reasonable because F dopants act as a defect-passivation agent as well.[13] For ZnO:Na-F, μ is slightly decreased to $63.07\,cm^2\ V^{-1}\ s^{-1}$ from $70.91\,cm^2\ V^{-1}\ s^{-1}$ for ZnO:F.

D. Photoluminescence characterization

The LT-PL spectra of undoped ZnO, ZnO:F, and ZnO:Na-F thin films are shown in Fig. 4. The intensities are normalized for clarity. All samples demonstrate a distinct ultraviolet (UV) near-band edge (NBE) emission [Fig. 4(a)]. The near-infrared (NIR) emission peaks at 1.6–1.7 eV are the second order of the UV NBE peaks. Note that except ZnO:F, both ZnO and ZnO:Na-F exhibit a quite broad visible emission band which is universally assigned to intrinsic or extrinsic defects, known as deep-level emission (DLE). The inset of Fig. 4(a) shows the raw spectra of the DLE region. The absence of the DLE peak in ZnO:F indicates that the deep level defects are mostly passivated.[23] Compared to the weak DLE band at ~2.3 eV in undoped ZnO, a more enhanced one is observed in ZnO:Na-F, which is ascribed to Zn vacancy (V_{Zn})-related defects.[24–28]

The fine structures of the NBE spectra are shown in Fig. 4(b). For undoped ZnO, the peak located at 3.370 eV corresponds to the free exciton (FX) recombination; the peak located at 3.356 eV (I_B) corresponds to the donor bound excitons (D^0X); the peak located at 3.311 eV corresponds to the donor-acceptor pair (DAP); and 3.234 eV and 3.165 eV are the photon replicas of DAP. The NBE band of ZnO:F (I_A, 3.381 eV) is broad, asymmetric, and blue-shifted due to the strong Burstein-Moss effect, which is quite typical for degenerated semiconductors.[29] For ZnO:Na-F, the peaks located at 3.311 eV and 3.234 eV are the same as those of undoped ZnO, and the one at 3.352 eV (I_C) corresponds to D^0X related to F donors. More details will be discussed below.

E. Discussion

The electron mobilities of ZnO:F and ZnO:Na-F are both larger than that of undoped ZnO, while the FWHM and RMS values are smaller. It is reported that F anions can passivate surface dangling bonds and diminish O-related defects.[11–13] According to these results, F dopants are beneficial for improving the crystalline quality of ZnO films, especially when codoped with Na.

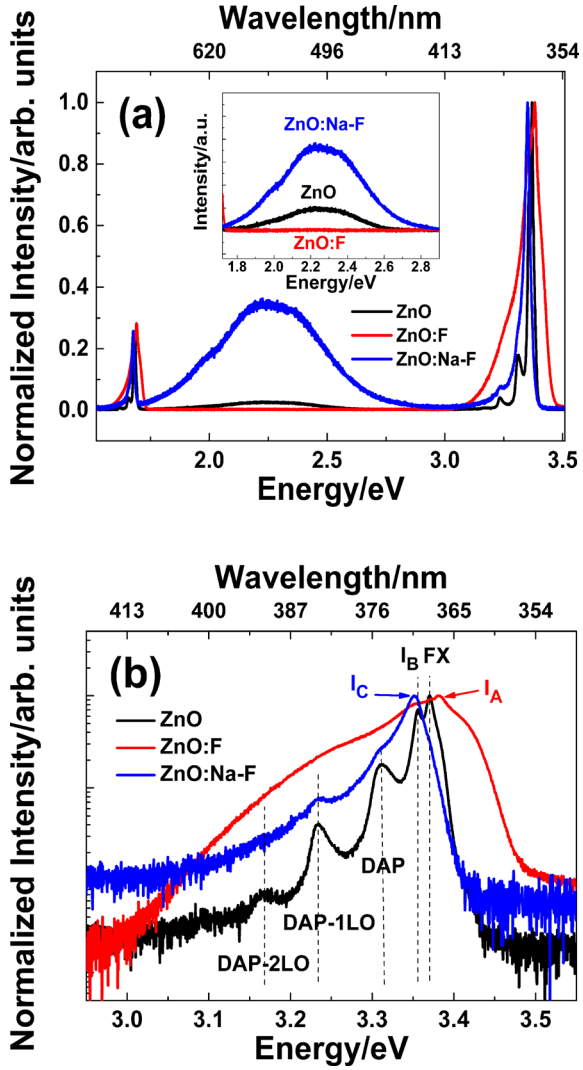

FIG. 4. Normalized LT-PL spectra of undoped ZnO, ZnO:F, and ZnO:Na-F thin films: (a) the full spectra and (b) the fine structures of the NBE region. The inset in (a) shows the raw spectra of the DLE region.

Although bound exciton peaks around 3.356 eV and 3.352 eV have been attributed to Na and Li acceptors, respectively,[30] their origins are still in debate. Actually, the peak at 3.352 eV (I_C) also exists as a shoulder in the PL spectrum of ZnO:F. Since the signal of Na is not detected in undoped ZnO or ZnO:F by SIMS, the I_C peak is reasonably attributed to D^0X caused by F donors. The DLE bands corresponding to 2.3 eV are supposed to originate from O vacancy (V_O) or V_{Zn}.[24–28,31–33] In the present study, all ZnO thin films are grown under O-rich conditions. Thus, the formation energy of V_O is high,[34] while that of V_{Zn} is low, suggesting that a large number of V_{Zn} exist in these ZnO films. Therefore, the DLE bands at 2.3 eV in undoped ZnO and ZnO:Na-F are ascribed to the electron transitions between the CBM or some shallow donor levels and V_{Zn} acceptor.

It has been well established that the formation energy of V_{Zn} would be decreased with the elevation of E_F,[1,35] and the

formation energy of V_O would be increased contrarily.[1,34] Note that degeneration happens in ZnO:F, evidenced by the broad, asymmetric, and blue shifted NBE [Fig. 4(b)],[29] thus a considerable number of V_{Zn} defects are generated as a consequence. However, the absence of the DLE band implies that most of the V_{Zn} acceptors are passivated, possibly by F donors. F atoms have a high volatility at 450 °C in ZnO,[36] and they occupy the anion sites, enabling them to readily migrate close to V_{Zn} and form $\left(F_O^+ - V_{Zn}^{2-}\right)^-$ complexes, as shown in Eq. (2). Liu *et al.*[23] found that the concentration of V_{Zn} increased as a function of Mg content in $Mg_xZn_{1-x}O$:F ($0 \le x \le 0.29$), and the DLE band appeared when $x \ge 0.12$. In the case of Ga-doped ZnO, where the Ga atoms occupy cation sites and diffuse slowly, Tang *et al.*[37] also found the relationship between V_{Zn} and the DLE band. When almost all of V_{Zn} were bounded in $\left(Ga_{Zn}^+ - V_{Zn}^{2-}\right)^-$ complexes, the position of DLE was at 650 nm (~1.9 eV). After annealing at 1023 K, a large number of complexes were dissociated, meanwhile, the concentration of V_{Zn} increased, and the DLE band shifted to 550 nm (~2.3 eV)

$$F_O^+ + V_{Zn}^{2-} \rightarrow \left(F_O^+ - V_{Zn}^{2-}\right)^-. \quad (2)$$

To quantitatively determine the degree of compensation (K) in ZnO:F, TDH measurements were carried out (see Fig. S1 in supplementary material). The μ vs T is fitted with D. C. Look's mobility model (see Fig. S2 and Appendix A in supplementary material),[38] which gives the concentrations of donor (N_D), F_O^+, and acceptor (N_A), $\left(F_O^+ - V_{Zn}^{2-}\right)^-$. For ZnO:F, $N_D = 1.47 \times 10^{20}\,cm^{-3}$ and $N_A = 4.31 \times 10^{19}\,cm^{-3}$, giving a K of 0.29 and an $[F]$ of $1.90 \times 10^{20}\,cm^{-3}$.

Na_i has not been observed in ZnO:Na-F from the XRD and XPS characteristics. Furthermore, an upper limit has been deduced from TDH measurement. First of all, there is an upper limit for the total concentration of ionized impurities $N_{ii} < 1.95 \times 10^{18}\,cm^{-3}$ (see Appendix B in supplementary material). Secondly, ZnO:Na-F may contain several kinds of ionized impurities, such as F_O^+, V_{Zn}^{2-}, $\left(F_O^+ - V_{Zn}^{2-}\right)^-$, Na_{Zn}^-, and Na_i^+, among which V_{Zn}^{2-} takes up a large percentage. Then, $[Na_i^+]$ is much less than N_{ii}. Lastly, [Na] is estimated to be $> 8.56 \times 10^{19}\,cm^{-3}$, and the percentage of interstitial Na is $[Na_i^+]/[Na] < 1.95 \times 10^{18}/8.56 \times 10^{19} \approx 2.3\%$. Note that this upper limit is overestimated, and the real percentage should be much less than 1%. During the growth of the ZnO:Na-F thin film, F doping will efficiently raise the E_F of ZnO films close to or above the CBM, leading to the formation energy of Na_i and Na_{Zn} increased and decreased, respectively. Therefore, the majority of Na dopants are in the form of Na_{Zn}, which compensates the electrons donated by F donors and causes a reduction of n.

On the other hand, the total concentration of impurities is over $10^{20}\,cm^{-3}$, two orders of magnitude higher than that of ionized impurities. Furthermore, the similar distribution profiles of Na and F in ZnO:Na-F suggest that the neighboring cation and anion dopants are bonded together. In this case, a large number of neutral $\left(F_O^+ - Na_{Zn}^-\right)^0$ complexes form due to the strong Coulomb interaction between F_O^+ and Na_{Zn}^-, as shown in Eq. (3). Besides, the formation of $\left(F_O^+ - Na_{Zn}^-\right)^0$ complexes leads to a great deal of isolated V_{Zn}, which gives rise to the strong DLE in the LT-PL spectrum of ZnO:Na-F

$$F_O^+ + Na_{Zn}^- \rightarrow \left(F_O^+ - Na_{Zn}^-\right)^0. \quad (3)$$

IV. CONCLUSION

In summary, single crystalline F-doped and Na-F codoped ZnO thin films have been successfully prepared by the rf-MBE method and the suppression of Na_i defect through Na-F codoping has been experimentally confirmed. F dopants benefit from the promotion of crystalline quality of ZnO films, resulting in higher mobility and smaller surface roughness. The amount of interstitial Na is estimated to be much less than 2.3% of the total Na impurities. As F doping efficiently raises the E_F of ZnO films, the formation of Na_i is consequently suppressed while most of the Na atoms reside on Zn sites, forming neutral $\left(F_O^+ - Na_{Zn}^-\right)^0$ complexes. The F donor in ZnO:F and ZnO:Na-F contributes to a D^0X luminescence at 3.352 eV. The DLE in ZnO:Na-F is remarkably enhanced due to the formation of $\left(F_O^+ - Na_{Zn}^-\right)^0$ complexes and a great deal of isolated V_{Zn}. Moreover, formation of $\left(F_O^+ - V_{Zn}^{2-}\right)^-$ complexes in ZnO:F exhausts most of the isolated V_{Zn} defects, leading to the disappearance of the DLE band. The codoping method may pave the way towards the realization of p-type ZnO materials.

SUPPLEMENTARY MATERIAL

See supplementary material for the temperature-dependent Hall data and the corresponding analyses.

ACKNOWLEDGMENTS

This work was supported by the National Natural Science Foundation of China (Grants Nos. 11674405, 11675280, 11274366, 51272280, and 61306011).

[1]A. Janotti and C. G. V. de Walle, Rep. Prog. Phys. **72**, 126501 (2009).
[2]T. C. Zhang, Y. Guo, Z. X. Mei, C. Z. Gu, and X. L. Du, Appl. Phys. Lett. **94**, 113508 (2009).
[3]C. H. Park, S. B. Zhang, and S.-H. Wei, Phys. Rev. B **66**, 073202 (2002).
[4]H. Shen, X. Zhao, L. Duan, R. Liu, H. Li, and B. Wang, J. Appl. Phys. **121**, 155303 (2017).
[5]E.-C. Lee and K. J. Chang, Phys. Rev. B **70**, 115210 (2004).
[6]J. Li, Y. Liu, Z. Mei, L. Vines, A. Kuznetsov, and X. Du, Mater. Sci. Semicond. Process. **69**, 28 (2017).
[7]T. Yamamoto and H. Katayama-Yoshida, J. Cryst. Growth **214–215**, 552 (2000).
[8]L. Chen, Z. Xiong, Q. Wan, and D. Li, J. Phys. Conf. Ser. **276**, 012158 (2011).
[9]R. D. Shannon, Acta Crystallogr. A **32**, 751 (1976).
[10]B. Liu, M. Gu, X. Liu, S. Huang, and C. Ni, Appl. Phys. Lett. **97**, 122101 (2010).
[11]J. Hu and R. G. Gordon, Sol. Cells **30**, 437 (1991).
[12]H. Y. Xu, Y. C. Liu, R. Mu, C. L. Shao, Y. M. Lu, D. Z. Shen, and X. W. Fan, Appl. Phys. Lett. **86**, 123107 (2005).
[13]Y.-J. Choi, K.-M. Kang, and H.-H. Park, Sol. Energy Mater. Sol. Cells **132**, 403 (2015).
[14]H. T. Yuan, Y. Z. Liu, Z. X. Mei, Z. Q. Zeng, Y. Guo, X. L. Du, J. F. Jia, Z. Zhang, and Q. K. Xue, J. Cryst. Growth **312**, 263 (2010).
[15]X. Du, Z. Mei, Z. Liu, Y. Guo, T. Zhang, Y. Hou, Z. Zhang, Q. Xue, and A. Y. Kuznetsov, Adv. Mater. **21**, 4625 (2009).

[16]Y. Chen, D. M. Bagnall, H. Koh, K. Park, K. Hiraga, Z. Zhu, and T. Yao, J. Appl. Phys. **84**, 3912 (1998).
[17]C. Dong, J. Appl. Crystallogr. **32**, 838 (1999).
[18]H. P. Klug and L. E. Alexander, *X-Ray Diffraction Procedures: For Polycrystalline and Amorphous Materials* (Wiley, 1974).
[19]R. R. Reeber, J. Appl. Phys. **41**, 5063 (1970).
[20]A. Tabib, W. Bouslama, B. Sieber, A. Addad, H. Elhouichet, M. Férid, and R. Boukherroub, Appl. Surf. Sci. **396**, 1528 (2017).
[21]A. Chelouche, T. Touam, F. Boudjouan, D. Djouadi, R. Mahiou, A. Bouloufa, G. Chadeyron, and Z. Hadjoub, J. Mater. Sci. Mater. Electron. **28**, 1546 (2017).
[22]S. Ghosh, G. G. Khan, S. Varma, and K. Mandal, ACS Appl. Mater. Interfaces **5**, 2455 (2013).
[23]L. Liu, Z. Mei, A. Tang, H. Liang, and X. Du, J. Phys. Appl. Phys. **50**, 065102 (2017).
[24]A. Janotti and C. G. Van de Walle, Phys. Rev. B **76**, 165202 (2007).
[25]T. M. Børseth, B. G. Svensson, A. Y. Kuznetsov, P. Klason, Q. X. Zhao, and M. Willander, Appl. Phys. Lett. **89**, 262112 (2006).
[26]M. A. Reshchikov, H. Morkoç, B. Nemeth, J. Nause, J. Xie, B. Hertog, and A. Osinsky, Phys. B Condens. Matter **401–402**, 358 (2007).
[27]M. A. Reshchikov, J. Q. Xie, B. Hertog, and A. Osinsky, J. Appl. Phys. **103**, 103514 (2008).
[28]C. Ton-That, L. Weston, and M. R. Phillips, Phys. Rev. B **86**, 115205 (2012).
[29]J. D. Ye, S. L. Gu, S. M. Zhu, S. M. Liu, Y. D. Zheng, R. Zhang, and Y. Shi, Appl. Phys. Lett. **86**, 192111 (2005).
[30]E. Tomzig and R. Helbig, J. Lumin. **14**, 403 (1976).
[31]K. E. Knutsen, A. Galeckas, A. Zubiaga, F. Tuomisto, G. C. Farlow, B. G. Svensson, and A. Y. Kuznetsov, Phys. Rev. B **86**, 121203 (2012).
[32]J. Lv and C. Li, Appl. Phys. Lett. **103**, 232114 (2013).
[33]S. Ghosh, G. G. Khan, A. Ghosh, S. Varma, and K. Mandal, CrystEngComm **15**, 7748 (2013).
[34]L. Liu, Z. Mei, A. Tang, A. Azarov, A. Kuznetsov, Q.-K. Xue, and X. Du, Phys. Rev. B **93**, 235305 (2016).
[35]A. Azarov, V. Venkatachalapathy, Z. Mei, L. Liu, X. Du, A. Galeckas, E. Monakhov, B. G. Svensson, and A. Kuznetsov, Phys. Rev. B **94**, 195208 (2016).
[36]F. Yakuphanoglu, Y. Caglar, S. Ilican, and M. Caglar, Phys. B Condens. Matter **394**, 86 (2007).
[37]A. Tang, Z. Mei, Y. Hou, L. Liu, V. Venkatachalapathy, A. Azarov, A. Kuznetsov, and X. Du, arXiv:1709.07603 [Cond-Mat] (2017).
[38]D. C. Look, K. D. Leedy, L. Vines, B. G. Svensson, A. Zubiaga, F. Tuomisto, D. R. Doutt, and L. J. Brillson, Phys. Rev. B **84**, 115202 (2011).